

Unsupervised Machine Learning with Independent Component Analysis to Identify Areas of Progression in Glaucomatous Visual Fields

Pamela A. Sample,¹ Catherine Boden,¹ Zuobua Zhang,^{2,3} John Pascual,¹ Te-Won Lee,³ Linda M. Zangwill,⁴ Robert N. Weinreb,⁴ Jonathan G. Crowston,⁴ Esther M. Hoffmann,⁴ Felipe A. Medeiros,⁴ Terrence Sejnowski,⁵ and Michael Goldbaum²

PURPOSE. To determine whether a variational Bayesian independent component analysis mixture model (vB-ICA-mm), a form of unsupervised machine learning, can be used to identify and quantify areas of progression in standard automated perimetry fields.

METHODS. In an earlier study, it was shown that a model using vB-ICA-mm can separate normal fields from fields with six different patterns of visual field loss related to glaucomatous optic neuropathy (GON) along maximally independent axes. In the present study, an independent group of 191 patient eyes (66 with ocular hypertension (OHT), 12 with suspected glaucoma by field, 61 with suspected glaucoma by disc, and 52 with glaucoma) with five or more standard visual fields under observation for a mean of 6.24 ± 2.65 years and 8.11 ± 2.42 visual fields were evaluated with the vB-ICA-mm. In addition, eyes with progressive GON (PGON) were identified ($n = 39$). Each participant had a series of fields tested, with each field entered independently and placed along the axes of the previously developed model. This allowed change in one pattern of visual field defect (along one axis) to be assessed relative to results other areas of that same field (no change along other axes). Progression was based on a slope falling outside the 5th and the 95th percentile limits of all slopes, with at least two axes not showing such a deviation in a given individual's series of fields. Fields were also scored using Advanced Glaucoma Intervention Study (AGIS) and the Early Manifest Glaucoma Treatment Trial (EMGT) criteria.

RESULTS. Thirty-two of 191 eyes progressed on vB-ICA-mm by this definition. Of the 32, 22 had field loss at baseline, 7 had only GON, 3 were OHTs and 12 were from the 39 eyes (31%) with PGON. The vB-ICA-mm identified a higher percentage of

progressing eyes in each diagnostic category than did AGIS or the EMGT.

CONCLUSIONS. The vB-ICA-mm can quantitatively identify progression in eyes with glaucoma by evaluating change in one or more patterns of the visual field loss while other areas or patterns remain stable. This may enable each eye to contribute to the determination of whether change is caused by true progression or by variability. (*Invest Ophthalmol Vis Sci.* 2005; 46:3684–3692) DOI:10.1167/iovs.04-1168

The importance of identifying progression has been highlighted by recent findings that show that treatment of glaucoma is effective in slowing progression of the disease.^{1–4} This finding has, in some ways, increased the difficulty of deciding when to begin treatment.⁵ In each of these studies, a different criterion for progression was used, and studies have shown little agreement among the different criteria for classifying an eye as having progressed.^{6,7}

However, it has been shown that the progression in visual fields occurs most commonly within or adjacent to areas that are already defective.^{8,9} Hence, a quantitative method that capitalizes on the defective pattern found within an individual's initial visual field could be helpful in facilitating the decision of when to instigate or change treatment.

In a companion study also published in this issue,¹⁰ we used the variational Bayesian independent component analysis mixture model (vB-ICA-mm) to develop a model that represents the structure of the patterns of visual field defects from 189 normal and 156 glaucomatous eyes. vB-ICA-mm used a form of unsupervised learning that separated the eyes into two groups—cluster G, with 107 of 156 patient eyes and 3 normal eyes, and cluster N, with 186 of 189 normal eyes plus 49 glaucomatous eyes—even though it had no indication of diagnosis or feedback from humans during training. The terms N and G are used to identify the clusters for the purposes of this report; however, the classifier at no time was given information about which diagnostic group a visual field belonged to.

Simultaneously, the classifier determined the optimal number of minimally dependent axes along which it could place the data within a cluster. The fields in cluster N required only one axis to describe them. The vB-ICA-mm placed the 107 glaucomatous and 3 normal eyes in cluster G along six axes. Post hoc analysis of the six axes and the associated standard automated perimetry (SAP) fields indicated that each axis was associated with a particular type of glaucomatous visual field defective pattern (Fig. 1). This analysis also showed that the pattern of loss for this cross-sectional data varied in severity along each axis. Fields were ordered by standard deviation (SD) from the mean of the eyes in cluster G. The positive SDs generally indicated more extreme defects, and the negative ones indicated smaller and less deep defects. To verify the direction of the SD, we assessed whether deeper defects also

From the ¹Visual Function and ²Ophthalmic Informatics Laboratories, the ⁴Hamilton Glaucoma Center, and the ³Institute for Neural Computation, Department of Ophthalmology, University of California, San Diego, La Jolla, California; and ⁵The Salk Institute, La Jolla, California.

Supported by National Eye Institute Grants EY08208 (PAS), EY13235 (MHG), Research to Prevent Blindness (PAS), and the Howard Hughes Medical Institute (TS).

Submitted for publication October 1, 2004; revised February 17 2005; accepted March 4, 2005.

Disclosure: P.A. Sample, Carl Zeiss Meditec, Inc. (F); C. Boden, None; Z. Zhang, None; J. Pascual, None; T.-W. Lee, None; L.M. Zangwill, None; R.N. Weinreb, Carl Zeiss Meditec, Inc. (F); J.G. Crowston, None; E.M. Hoffmann, None; F.A. Medeiros, None; T. Sejnowski, None; M. Goldbaum, None

The publication costs of this article were defrayed in part by page charge payment. This article must therefore be marked "advertisement" in accordance with 18 U.S.C. §1734 solely to indicate this fact.

Corresponding author: Pamela A. Sample, PhD, Department of Ophthalmology, University of California, San Diego, 9500 Gilman Drive, La Jolla, CA 92093-0946; psample@glaucoma.ucsd.edu.

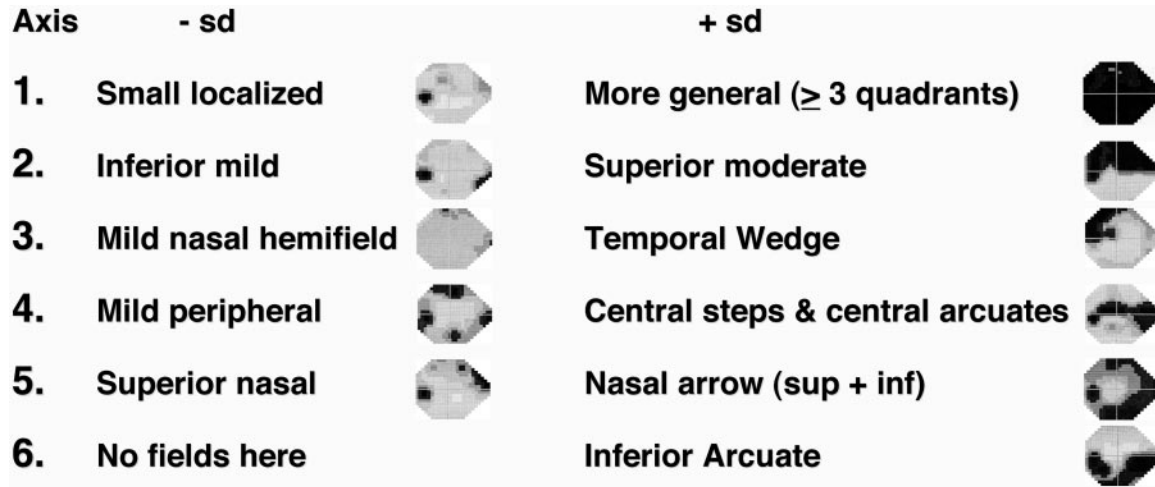


FIGURE 1. Examples of the fields found near the ends along both the + and - directions of each of the six axes identified in the original vB-ICA-mm space¹⁰ with descriptions for each. Note that fields can be progressing in both + and - SD directions if they are also moving away from the cluster G mean.

moved away from the mean of cluster N while shallower defects moved toward it (Fig. 2). To summarize, the classifier organized the fields in multidimensional space based on both the pattern of the visual field defect and its severity.

For the present study, we evaluated whether this unsupervised model could be used to place serial visual fields from an independent set of eyes within this multidimensional space for the purpose of identifying progression. In this analysis, we posed two questions: Can a change in serial fields be detected from one individual in whom a defect is progressing within a particular pattern of visual field loss (i.e., along one axis)? And, can the lack of change along the other axes (i.e., for other patterns of field loss) be used to account for variability in the individual patient, to verify that the change is real? If so, this method could help surmount the ongoing clinical problem of

accurate identification of true glaucomatous progression in visual fields when fluctuations due to learning effects, fatigue, and changes in the physiological state of the eye and the long-term fluctuation inherent in psychophysical testing are also present.¹¹⁻¹³

METHODS

Subjects

The visual field data came from a 14-year longitudinal study of visual function in glaucoma: The Diagnostic Innovations in Glaucoma Study (DIGS) at the Hamilton Glaucoma Center, University of California at San Diego. One eye of each of 191 patient participants was included. None of these participants was used in the original dataset of 345 eyes

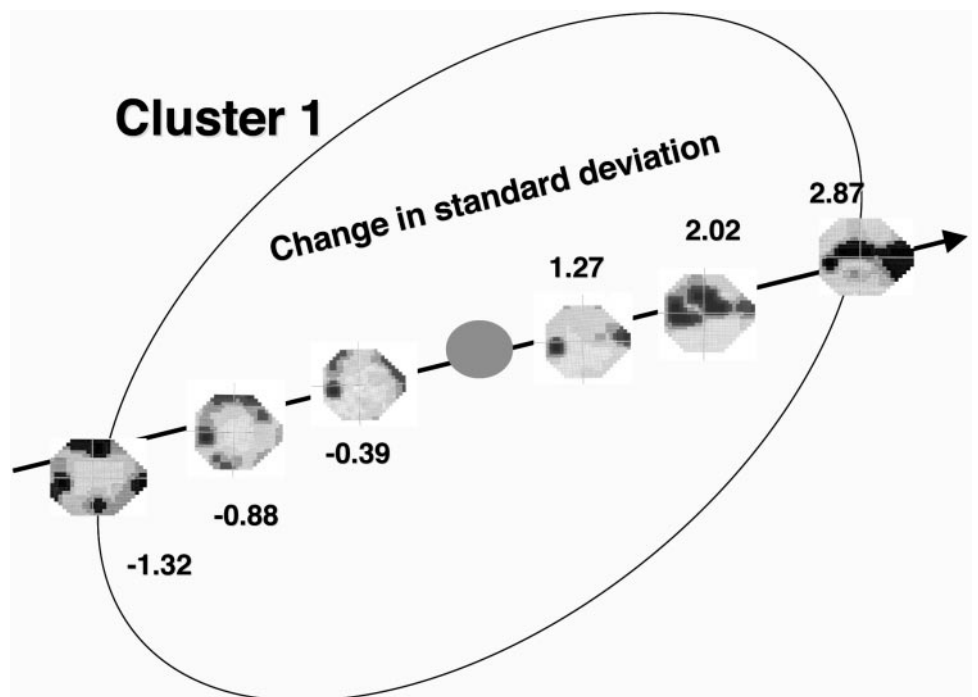


FIGURE 2. Example of fields at various SDs along axis 4 from cluster 1 in the original vB-ICA-mm space. The patterns of loss remain similar in the + and - directions with increasing severity of defect with increasing SD.

TABLE 1. Diagnostic Categories and Criteria

Diagnostic Category	Visual Field CPSD at 5% or GHT ONL	Stereophoto Grade GON	IOP >22 mm Hg Twice	<i>n</i>
Ocular hypertension	No	No	Yes	66
Suspect by disc	No	Yes	Yes or No	61
Suspect by field	Yes	No	Yes or No	12
Glaucoma	Yes	Yes	Yes or No	52

cpsd, corrected pattern standard deviation; GHT, glaucoma hemifield test; ONL, outside normal limits.

to create the model. Informed consent was obtained from all participants after the nature and possible consequences of the study were explained. The Institutional Review Board of the University of California at San Diego approved the study, which complied with the tenets of the Declaration of Helsinki.

Inclusion Criteria for DIGS

Simultaneous stereoscopic fundus photographs were obtained of all subjects and were of adequate quality for the subject to be included. All subjects had open angles, best corrected acuity of 20/40 or better, spherical refraction within ± 5.0 D, and cylinder correction within ± 3.0 D. A family history of glaucoma was allowed. One eye was randomly selected for testing.

Exclusion Criteria for DIGS

Ocular hypertensive subjects were excluded if they had a history of intraocular surgery (except for uncomplicated cataract surgery). We also excluded all subjects with nonglaucomatous secondary causes of elevated IOP (e.g., iridocyclitis or trauma), other intraocular eye disease, other diseases affecting the visual field (e.g., pituitary lesions, demyelinating diseases, HIV positivity or AIDS, or diabetic retinopathy), medications known to affect visual field sensitivity, or problems that affect color vision other than glaucoma.

Criteria for The Current Study

Exclusion criteria for visual fields included unreliable visual fields (defined as any one of either fixation loss, false-negative, or false-positive errors $\geq 33\%$, unless false negatives could be explained by significant field loss). Only subjects with five or more standard visual fields in a series were included.

Participants ($n = 191$) were placed in one of four diagnostic categories based on the appearance of the optic disc (as described later) and on the presence or absence of repeatable visual field defects at baseline (Table 1). Ocular hypertensive eyes had IOPs of more than 22 mm Hg on at least two occasions, with normal-appearing optic discs and normal visual fields. Eyes suspected of glaucoma by disc characteristics had normal visual fields, but evidence of glaucomatous optic neuropathy (GON). Those suspected by field defect had no evidence of GON, but had visual field that repeatedly showed abnormality. Patients with primary open-angle glaucoma (POAG) had both evidence of GON and repeatable abnormal visual fields.

Color simultaneous stereoscopic photographs were obtained (TRC-SS camera; Topcon Instrument Corp. of American, Paramus, NJ) after maximum pupil dilation. Stereoscopic disc photographs were recorded for all patients within 6 months of the field test result in the baseline data set. Photographs were independently assessed by two trained masked graders using a stereoscopic viewer (Pentax Stereo Viewer II; Asahi, Tokyo, Japan) illuminated with color-corrected fluorescent lighting. Glaucomatous optic neuropathy was defined by evidence of any of the following: excavation, neuroretinal rim thinning or notching, nerve fiber layer defects, or an asymmetry of the vertical cup-to-disc ratio ≥ 0.2 between the two eyes. Inconsistencies between the two graders' evaluations were resolved by consensus or through adjudication by a third evaluator.

In addition, we did a secondary analysis of the above individuals to determine whether there was any history of progressive GON (PGON) at any time during follow-up, as a more stringent definition of glaucoma. To identify progressive GON, the first and last photographs in each participant's series of photographs were graded by two independent masked reviewers. The dates of the photographs were masked, and each reviewer was required to state whether A was more advanced than B, B more than A, or no change. A and B are assigned randomly within each pair of photographs. Inconsistencies between the two graders' evaluations were resolved through adjudication by a third evaluator.

Visual Field Testing

All subjects had automated full-threshold standard visual field testing with (Humphrey Visual Field Analyzer; Carl Zeiss Meditec Inc., Dublin, CA) with program 24-2 or 30-2. The visual field locations in program 30-2 that are not in program 24-2 were deleted from the data and display. Visual fields were classified as abnormal when a corrected pattern standard deviation was triggered at the 5% value or worse or the Glaucoma Hemifield Test result was outside normal limits. Two abnormal fields in sequence were required for classification as suspect by field or POAG.

The vB-ICA-mm

The complete methods for the vB-ICA-mm are given in the companion article.¹⁰ In brief, vB-ICA-mm was used as an unsupervised classifier on the SAP data. vB-ICA-mm identifies the number of clusters and the number of axes in each cluster. Each cluster is then examined and labeled according to the majority of positive-negative data points within. vB-ICA-mm finds the number of clusters and the number of axes in each cluster. For each number of clusters, c ($c = 1, 2$), and each number of axes, m ($m = \text{up to } 20$), it does the following:

Step 1: It randomly divides the data into c clusters

Step 2: For each cluster, it looks for a set of m axes that are maximally independent to describe that cluster.

Step 3: It adjusts the clustering membership of each data point so that the marginal likelihood is maximized. The marginal likelihood is defined as $P(X|H) = \int P(X|\theta, H)P(\theta|H)d\theta$, in which X stands for the dataset, H is the model, and θ is the parameters of the model. $P(\theta|H)$ is the prior distribution of θ in model H .

The vB-ICA-mm then iterates between steps 2 and 3 until there is no change in the cluster assignment. The vB-ICA-mm was set to repeat the initial randomization (step 1) 100 times, so that for each c and m , we had 100 models. All the above was repeated while the number of clusters and the number of axes were simultaneously varied. We chose the final model by comparing all the models based on their marginal likelihood values (the larger the value, the better) and the classification accuracy. The chosen model was then used for this report to assess each of the serial visual fields from the 191 participants.

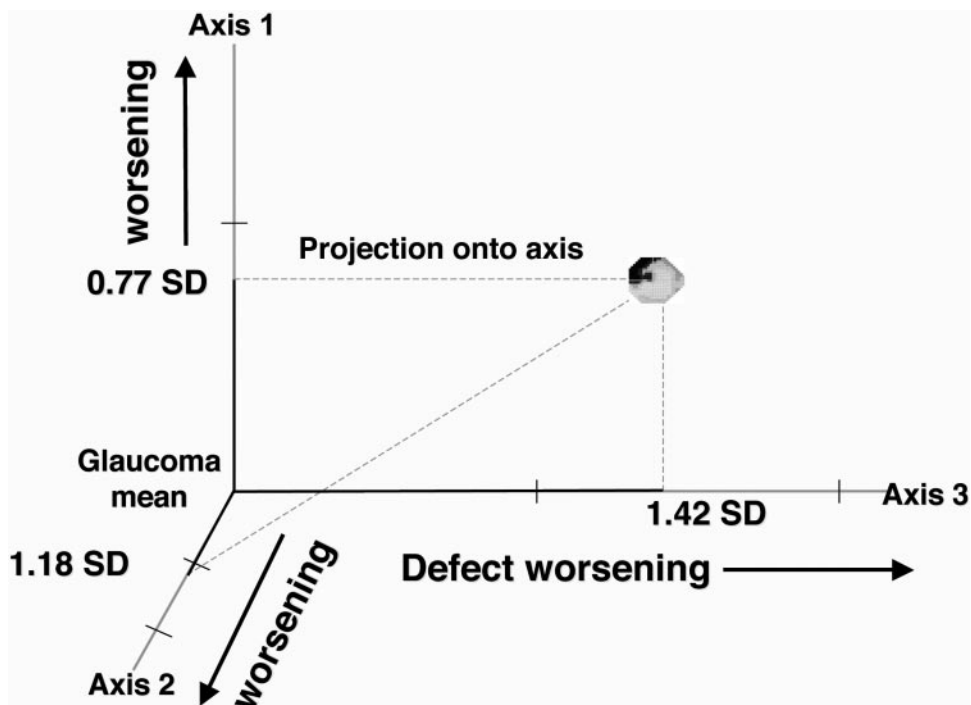


FIGURE 3. One field from a series of fields from a patient in this study. Each field in the series is projected independently to each of the six axes of the original vB-ICA-mm space. Only three axes are shown here for clarity. In this depiction, this particular field would be most strongly associated with axis 3 at this point in the original vB-ICA-mm space.

The input to the machine learning classifier included age and the absolute sensitivity in decibels of each of the 52 test locations (not including two locations near the blind spot) in the 24-2 visual field. These were the same input values used in the companion study, which developed the axes and analyses used in the present study. The 52 threshold values were extracted from the perimeter (Peridata 6.2 program; Peridata Software GmbH, Hürth, Germany). Age was provided because it is an important correction factor used in visual field analysis.

In the original vB-ICA-mm, six minimally dependent axes were optimal to describe the cluster holding most of the visual fields from eyes with GON. All six axes passed through the mean of that cluster generated by the classifier. The distance of each visual field from this mean along a given axis was computed in SD units. This allowed each field to be plotted in multidimensional space (Fig. 3). In the original study using cross-sectional data, each field was associated with a particular axis by calculating the angle at the cluster centroid between the vector for that field and the vector of each of the axes. The individual field was assigned to the axis with which the SAP vector had the smallest angle. In the present study in serial visual fields, each visual field was projected onto the multidimensional space specified by the vB-ICA-mm developed in our prior study. At the same time, the relationship of the field to all six axes was maintained. Each field was placed along each axis according to the projection onto the axis in units of the SD from the mean of the glaucoma group (Fig. 3). The temporal relationship among all the fields in a given patient's series were then evaluated by post hoc analysis.

Post Hoc Analyses of Change

To classify a field series as progressing or not, we analyzed the changes in projections over time along each of the six axes with linear regression. The slope of each regression line indicates how fast the change was occurring. To identify change along a given axis, we pooled all the slopes of all the patients along all six axes. If a slope was outside percentiles 95, 97.5, or 99 on an axis, we considered it to be a change only if there were at least two axes that did not show such a change

(e.g., the slope fell within the 95% limits (see the Discussion section). Figure 4A shows the results for one participant. The arrows indicate the actual plotted SDs and the associated regression line (dark line) where the slope is outside the percentile bands (pale lines) for a given axis. Please note that, in the model, movement in the negative-SD direction indicates either progression or improvement.¹⁰

To separate changes associated with progressing visual fields from change associated with improving visual fields, we also assessed whether serial fields were moving closer in space to the mean of cluster N, the cluster that held 98.9% of the normal eyes from our previous study. If so, that would indicate improvement. If the fields were moving away from both the cluster N and G means, it would indicate progression.

We also assessed whether the fields from a given individual's series of fields switched cluster assignment or axis assignment over time. Initial cluster assignment required the first two fields in a series to be in the original cluster and three successive follow-up fields to switch to the other cluster. A switch in axis involved moving from the designated baseline axis (the one with the smallest angle to the SAP vector) to a second axis for three or more subsequent consecutive fields.

Finally, to put the results into a clinical perspective, we graded each individual's series of fields by using the scoring procedures from two major clinical trials, the Advanced Glaucoma Intervention Study (AGIS)¹ and the Early Manifest Glaucoma Treatment (EMGT) trial.¹⁴

The AGIS algorithm was developed to determine eligibility for the AGIS study and to evaluate visual field progression in patients with advanced glaucoma. Very briefly, the AGIS score is calculated by totaling the number of adjacent depressed test locations on the total deviation plot found in the upper, lower, and nasal hemifields of a standard visual field. The final AGIS score for each field ranges from 0 to 20. Progression requires an increase in score of ≥ 4 points between the average score of the two baseline visual fields and the score on each of three consecutive follow-up fields.

The EMGT was designed to compare the effect of immediate therapy with lower IOP versus late or no treatment on the progression of newly diagnosed early glaucoma. The progression algorithm for the EMGT is a modification of the Glaucoma Change Probability (GCP)

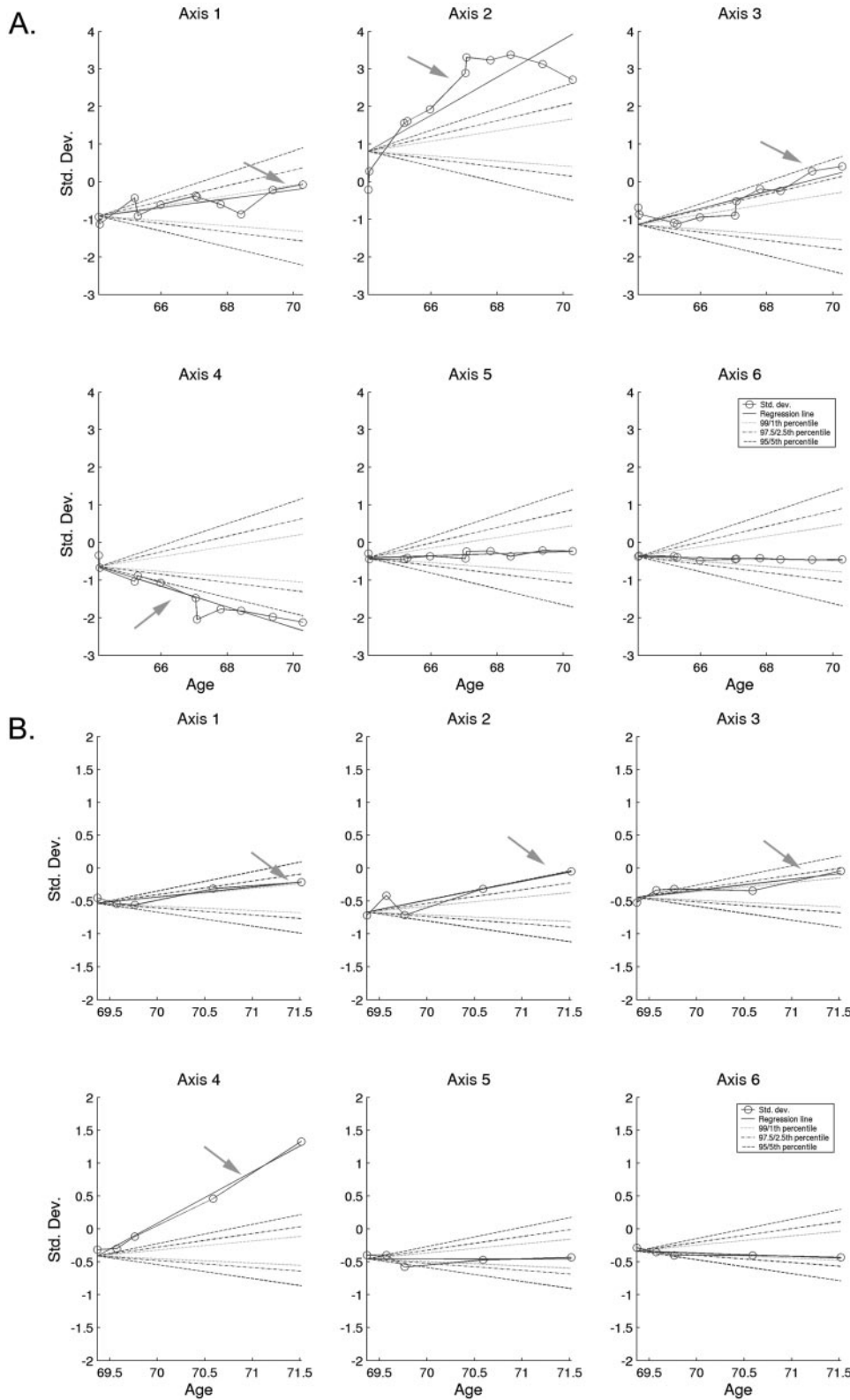


FIGURE 4. Each box holds axis results for the entire set of fields from a patient. The pale lines depict percentile ranges 95, 97.5, and 99 ranges. The wavy lines are the actual result of the classification and the darker straight line is the regression line fit to the data. *Arrows within each axis panel: data falling outside the percentile limits for no change (i.e., progression).* (A) Results from a patient with visual field loss without GON; (B) an ocular hypertensive; (C) a patient with GON and no visual field loss; and (D) a patient with GON and visual field loss. Note that for this participant, there was a 5-year interval between the first and second field tests, which might exaggerate change along the axis. Change would disappear if the first field were not included. This time lapse does not mean, however, that there was no progression between the first and second field tests. A review of the actual fields shows on field 1 a nasal step on the pattern deviation plot encompassing five points at $P < 0.05$ and one at $P < 0.01$. The second field shows a full arcuate defect that included those six points all at $P < 0.05$. This participant was lost to the study during the break between field tests, but a review of the medical records showed that the physician noted progression and performed an argon laser trabeculoplasty in 1989. In 1992 he noted a disc hemorrhage, progression and did a trabeculectomy. The patient's glaucoma was considered stable for the remainder of the years through 1998.

analysis commercially available on the Humphrey Visual Field Analyzer (Carl Zeiss Meditec, Inc.). The GCP uses the total deviation plot values and the EMGT uses pattern deviation plot values. Progression with the EMGT criteria requires deterioration in at least three of the same locations on three consecutive follow-up field tests.

RESULTS

The mean follow-up was 6.24 ± 2.65 years with a mean number of fields of 8.11 ± 2.42 (range, 5-17). Mean age at baseline was 61.03 ± 12.15 years (range, 25.3-87.5). Table 2

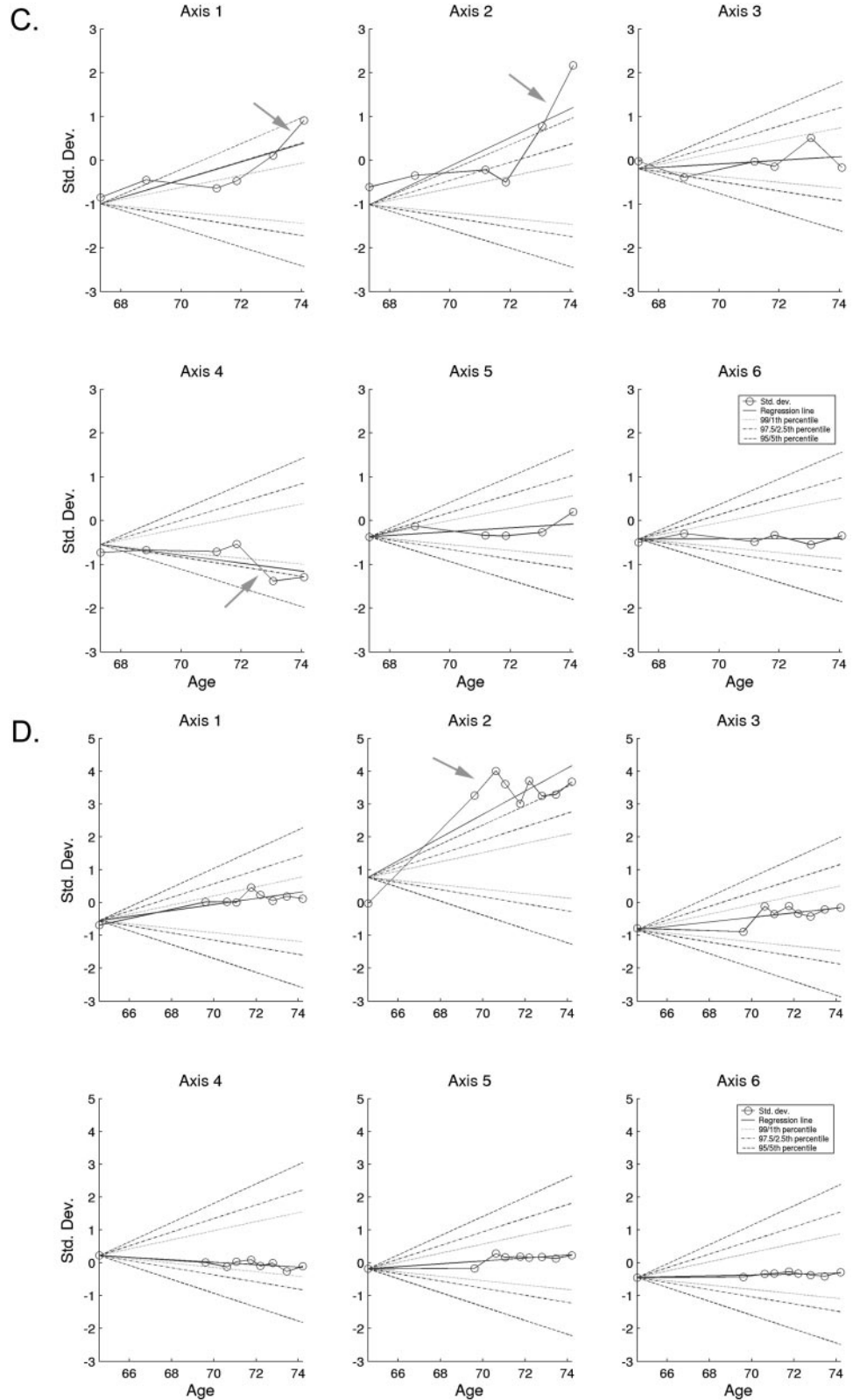


FIGURE 4. (Continued)

gives the number of participants progressing at each percentile cutoff (only the most stringent cutoff is recorded for each participant). The total progressing and percentage are also given within each diagnostic category. The fewest progressors were in the ocular hypertensive group (3/66 = 5%), followed

by 7 (11%) of 61 with GON and normal fields, 5 (42%) of 12 with field loss only, and 17 (33%) of 52 with visual field loss and GON. Thirty-nine of the 191 eyes had progressive GON, and 12 (31%) of 39 were identified by the vB-ICA-mm as having progressive disease.

TABLE 2. Number Progressing at Mutually Exclusive Percentiles by Diagnostic Category

Diagnosis	<i>n</i>	95%	97.5%	99%	Total	%
Ocular hypertension	66	1	0	2	3	5
GON without VF loss	61	2	3	2	7	11
VF loss without GON	12	0	4	1	5	42
VF and GON	52	9	3	5	17	33
Total	191	12	10	10	32	17
Progressing GON	39	6	4	2	12	31

VF, visual field.

It was also possible for participants to change cluster assignment or axis assignment. A change in cluster assignment was rare (11/191 eyes) with nine changing from cluster N (the cluster associated most strongly with normal eyes) to cluster G (the cluster holding mostly patient eyes). Six of these were eyes with GON and no visual field loss at baseline. Only two eyes changed from cluster G to cluster N.

Ten of the 32 eyes that progressed changed axis assignment. In all cases, the initial axis assignment was within ± 0.43 SDs of the axis they switched to (see e.g., Fig. 4B), and in all but one case, the switch was to an axis showing progression.

Table 3 gives the number of participants with changes according to axis. Results of the vB-ICA-mm for four participants are shown in Figure 4. No change in SD outside the percentile limits on at least two axes was required before change within a given pattern along an axis was considered to show progression. This, along with the requirement of a significant slope outside the bounds of the percentile limits, strengthens the determination that the change is due to progression and not to the patient's variability. Figure 5 shows the actual visual field gray scales for two participants in the study, the ones also shown in Figures 4A and 4B.

Figure 6 gives the results of the two clinical criteria for progression compared with the vB-ICA-mm for comparison. The vB-ICA-mm identified a higher percentage of progressing eyes in each diagnostic category. Figure 7 shows agreement among the vB-ICA-mm, AGIS, and EMGT.

DISCUSSION

Although there have been numerous reports on techniques for monitoring progression in glaucomatous visual fields with several good reports of currently used strategies,¹⁵⁻¹⁷ to our knowledge, only two other studies have used machine classifiers to look at progression of visual fields.^{18,19} Henson et al.¹⁸ used a Kohonen self-organizing map to classify fields based on the pattern and severity of defect. The emphasis on pattern and severity is similar to our approach, but while Henson et al. gave examples of how this approach might be used for progression, they did not analyze serial fields from their participants. However, an important component of their study was to use mod-

eling techniques to estimate the test-retest variability unrelated to progression. We chose to handle this by comparison of change along one or more axes (essentially a deepening or expansion of a specific pattern of defect) while at least two other axes remained stable. This allows the individual's own variability in real time to contribute to the evaluation rather than relying on estimates from other individuals. One drawback to our approach could be that areas of the field with a defect are thought to be more variable than areas closer to normal. We could misinterpret as progression changes due to the increased variability in axes with more defect relative to the stability on axes representing still normal areas of the visual field. However, we think this possibility is outweighed by the information gained on the particular individual's variability field by field and the stringent criteria requiring the slope to fall outside the percentile limits derived from the whole group. If we had had an independent sample of stable eyes with serial visual field results to develop the percentile limits, it is likely we could have found more evidence of progression; we plan to do this in the future.

Brigatti et al.¹⁹ used a three-layer back-propagation neural network to assess progression in serial fields. A drawback to their study was the use of AGIS scoring as the gold standard for progression. As noted before, there is no agreement on such a standard. Finally, both Brigatti et al.¹⁹ and Henson et al.^{18,20} used supervised learning, that trained the classifiers to identify progression based on AGIS criteria in the first case and defined defects with variability modeling in the second case. The vB-ICA-mm is unsupervised and classifies the data without any training or biases. Its effectiveness in this study could be assessed in the post hoc analyses after the classifier has finished. The specificity of 98.9% shown in our companion study¹⁰ and the logical distribution of progressed eyes within the different diagnostic groups of this study (Table 2) suggest that the vB-ICA-mm is classifying both defects and progression in a manner consistent with clinical expectations. For example, this study found the smallest percentage progressing in the OHT group, 5% (3/66). An estimate falling within those in the Ocular Hypertension Treatment Study of 4.4% in the treated group and 9.5% in the untreated group.³ The vB-ICA-mm found 33% to 42% of patients with baseline field loss progressing, which is similar to the 45% in the EMGT's treated group.²¹ Thirty-one percent of eyes with progressing GON were also identified by the vB-ICA-mm as progressing. This logical breakdown provides some evidence to address the concern that the vB-ICA-mm may be overcalling progression. Although the classifier is finding more eyes progressing than either AGIS or EMGT, the correspondence with the eyes also showing progressive GON is much stronger for vB-ICA-mm (31% compared with 15% by EMGT and 17% by AGIS). It has been shown that AGIS and EMGT often do not agree in their determination of progression.^{6,7} However, continued work is necessary to determine the true predictive ability of the vB-ICA-mm relative to other algorithms.

TABLE 3. Number of Participants with Changes along Each Axis

Axis	Defect (−SD)	Defect (+SD)	<i>n</i>
1	Small localized	More general (≥ 3 quadrants)	18
2	Inferior mild	Superior moderate	9
3	Mild nasal hemifield	Temporal wedge	11
4	Mild peripheral	Central steps and central arcuates	9
5	Superior nasal	Nasal arrow (sup + inf hemifields)	9
6	No fields	Inferior arcuate	5

Sup, superior; inf, inferior.

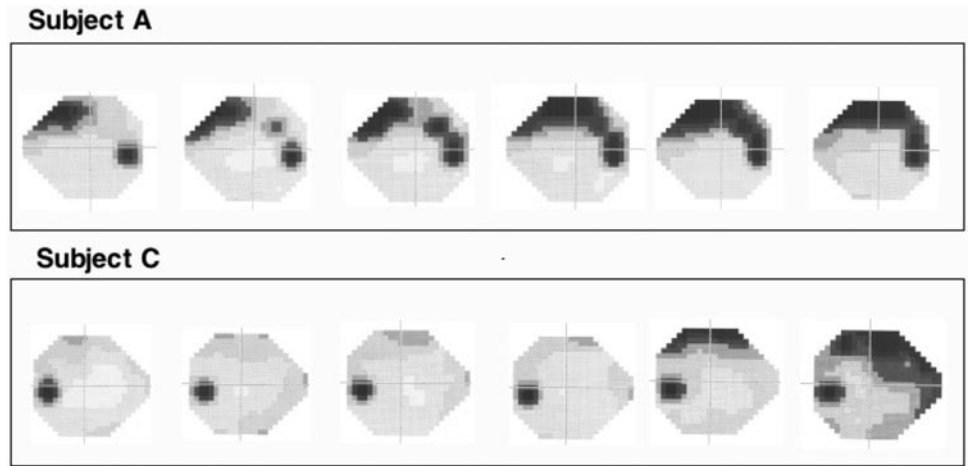


FIGURE 5. The gray scale printouts for the entire series of fields, all of which fell within the positive SD direction in subjects A (Fig. 4A) and C (Fig. 4B). These depict the pattern of defect and its progression over time.

In addition, it was rare that individuals switched clusters (i.e., they remained in the mostly glaucoma cluster). Axis assignment over time also generally remained stable, suggesting that the classifier is consistent in its determinations. The exception to this was in individuals who had more than one possible pattern at baseline, but as progression occurred the slightly less obvious one became more and more apparent. We could take into account change along more than one axis as shown in the figures.

More work is needed to optimize the strategies for defining rate or event of progression using this technique. In our first pass with a post hoc analysis of the results using the vB-ICA-mm approach to look at progression, we decided to be as conservative as possible about the definition of progression. The SD does reflect a degree of change along a particular axis that is associated with the range of severity found along that axis. This could eventually allow a quantifiable estimate of progression as an event. At this point, however, we decided to rely on a definition based on linear regression. Pooling the slopes from all axes caused the percentile limits for progres-

sion to be derived from those patients showing the greatest progression. This conservative approach most likely underestimated the number progressing according to vB-ICA-mm.

Each of the sponsored clinical trials using progression algorithms^{1,3,4,22} required a minimum of five visual fields before progression could be assessed: two baseline fields plus three shown in repeated tests to be progressing. The vB-ICA-mm was also able to identify progression with as few as five fields using a quantifiable change on some axes while at least two remained stable. It did this based on the slope of the change and did not require any other a priori definition of progression.

In summary, the main advantage of the vB-ICA-mm for identifying progression is that the definition for progression arises from the classification based on pattern of defect and the quantifiable distance along particular axes in space as the field progresses. This approach incorporates fewer biases. It provides a quantifiable means for making an assessment in serial visual fields, and it allows the individual's own variability to be somewhat taken into account to make the distinction between true progression versus variability.

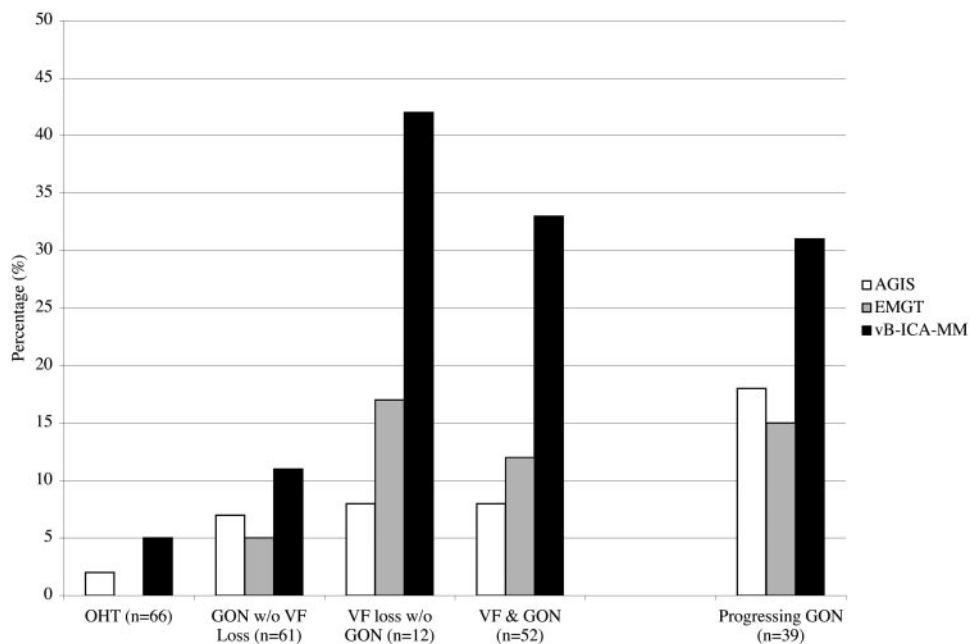


FIGURE 6. Histograms showing the percentage of eyes identified as having progressed in each diagnostic category using the AGIS, EMGT, and vB-ICA-mm criteria.

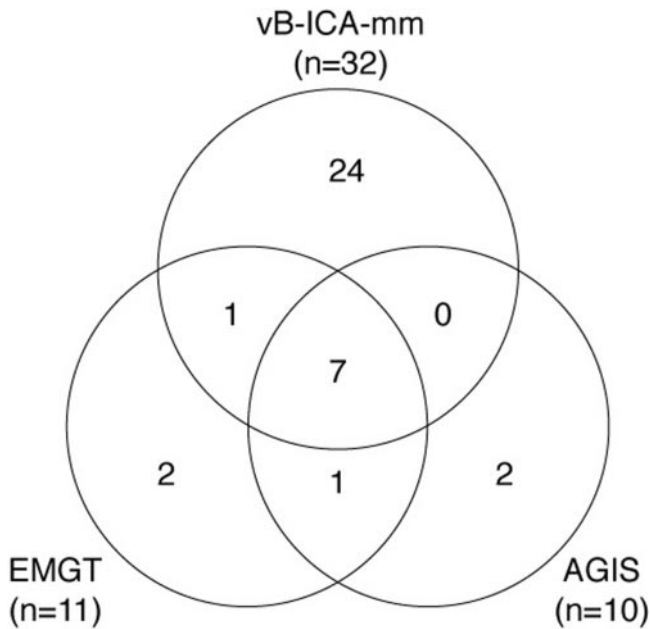


FIGURE 7. A Venn diagram showing the agreement among the three progression algorithms: EMGT, AGIS, and vB-ICA-mm.

Acknowledgments

The authors thank the AGIS and EMGT investigators and Carl Zeiss Meditec for providing the software to complete the scoring of visual fields.

References

1. The Advanced Glaucoma Intervention Study (AGIS). 7. The relationship between control of intraocular pressure and visual field deterioration. *Am J Ophthalmol*. 2000;130:490-491.
2. Higginbotham EJ, Gordon MO, Beiser JA, et al. The Ocular Hypertension Treatment Study: topical medication delays or prevents primary open-angle glaucoma in African American individuals. *Arch Ophthalmol*. 2004;122:813-820.
3. Kass MA, Heuer DK, Higginbotham EJ, et al. The Ocular Hypertension Treatment Study: a randomized trial determines that topical ocular hypotensive medication delays or prevents the onset of primary open angle glaucoma. *Arch Ophthalmol*. 2002;120:701-713.
4. Heijl A, Leske MC, Bengtsson B, et al. Reduction of intraocular pressure and glaucoma progression: results from the Early Manifest Glaucoma Trial. *Arch Ophthalmol*. 2002;120:1268-1279.
5. Robin AL, Frick KD, Katz J, Budenz D, Tielsch JM. The ocular hypertension treatment study: intraocular pressure lowering prevents the development of glaucoma, but does that mean we should treat before the onset of disease? *Arch Ophthalmol*. 2004;122:376-378.
6. Katz J, Congdon N, Friedman DS. Methodological variations in estimating apparent progressive visual field loss in clinical trials of glaucoma treatment. *Arch Ophthalmol*. 1999;117:1137-1142.
7. Lee AC, Sample PA, Blumenthal E, Berry C, Zangwill L, Weinreb RN. Infrequent confirmation of visual field progression. *Ophthalmology*. 2002;109:1059-1065.
8. Mikelberg F, Drance SM. The mode of progression of visual field defects in glaucoma. *Am J Ophthalmol*. 1984;98:443-445.
9. Boden C, Blumenthal EZ, Pascual J, et al. Patterns of glaucomatous visual field progression identified by three progression criteria. *Am J Ophthalmol*. 2004;138:1029-1036.
10. Goldbaum MH, Sample PA, Zhang Z, et al. Using unsupervised learning with independent component analysis to identify patterns of glaucomatous visual field defects. *Invest Ophthalmol Vis Sci*. 2005;46:3676-3683.
11. Flammer J, Drance SM, Zulauf M. Differential light threshold: short- and long-term fluctuation in patients with glaucoma, normal controls, and patients with suspected glaucoma. *Arch Ophthalmol*. 1984;102:704-706.
12. Wild JM, Searle AET, Dengler-Harles M, O'Neill EC. Long-term follow-up of baseline learning and fatigue effects in automated perimetry of glaucoma and ocular hypertensive patients. *Acta Ophthalmol*. 1991;69:210-216.
13. Birch MK, Wishart PK, O'Donnell NP. Determining progressive visual field loss in serial Humphrey visual fields. *Ophthalmology*. 1995;102:1227-1234; discussion 1234-1235.
14. Leske MC, Heijl A, Hussein M, et al. Factors for glaucoma progression and the effect of treatment: the early manifest glaucoma trial. *Arch Ophthalmol*. 2003;121:48-56.
15. Nouri-Mahdavi K, Hoffman D, Coleman AL, et al. Predictive factors for glaucomatous visual field progression in the advanced glaucoma intervention study. *Ophthalmology*. 2004;111:1627-1635.
16. Spry PGD, Johnson CA. Identification of progressive glaucomatous visual field loss. *Surv Ophthalmol*. 2002;47:158-173.
17. Vesti E, Johnson CA, Chauhan BC. Comparison of different methods for detecting glaucomatous visual field progression. *Invest Ophthalmol Vis Sci*. 2003;44:3873-3879.
18. Henson DB, Spenceley SE, Bull DR. Artificial neural network analysis of noisy visual field data in glaucoma. *Artif Intell Med*. 1997; 10:99-113.
19. Brigatti L, Nouri-Mahdavi K, Weitzman M, Caprioli J. Automatic detection of glaucomatous visual field progression with neural networks. *Arch Ophthalmol*. 1997;115:725-728.
20. Henson DB, Spenceley SE, Bull DR. Spatial classification of glaucomatous visual field loss. *Br J Ophthalmol*. 1996;80:526-531.
21. Heijl A, Lindgren G, Lindgren A, et al. Extended empirical statistical package for evaluation of single and multiple fields in glaucoma: Statpac 2. *Perimetry Update*. Amsterdam: Kugler & Ghedini; 1991:303-315.
22. Musch DC, Lichter PR, Guire KE, Standardi CL. The Collaborative Initial Glaucoma Treatment Study: study design, methods, and baseline characteristics of enrolled patients. *Ophthalmology* 1999; 106:653-662.